cold neutron triple axis spectrometer **SIKA** has high-energy resolution and allows researchers to probe this small difference in the location of the spin dynamics. The chopper spectrometer 4SEASONS at J-PARC was used to observe high-energy modes of the itinerant electron model. These inelastic neutron scattering experiments provided valuable insight into the fundamental physics of magnetism. (Reported by Shinichiro Yano)

*This report features the work of Song Bao and his collaborators published in Phys. Rev. X **12**, 011022 (2022).*

ANSTO SIKA – Cold Neutron Triple-axis Spectrometer

- Neutron Inelastic Scattering
- Materials Science, Condensed-matter Physics

Reference

1. S. Bao, W. Wang, Y. Shangguan, Z. Cai, Z.-Y. Dong, Z. Huang, W. Si, Z. Ma, R. Kajimoto, K. Ikeuchi, S.-I. Yano, S.-L. Yu, X. Wan, J.-X. Li, J. Wen, Phys. Rev. X **12**, 011022 (2022).

Determining the Structures of Photoresponsive Polymers Using Small-Angle Neutron Scattering

An azobenzene-containing polymer provides tunable structures and a unique performance under an external stimulus, which enables it to be used as a light-controllable nanocarrier for drug delivery.

Chieh-Tsung Lo's group in National Cheng Kung University, Taiwan, prepared an azobenzene-containing triblock copolymer, poly(6-[4-(4′-ethoxyphenylazo)phenoxy]hexyl methacrylate)-block-poly(ethylene glycol)-block-poly(6-[4-(4′-ethoxyphenylazo)phenoxy]hexyl methacrylate) (PMMAzo-b-PEG-b-PMMAzo), and developed a relation between its structures and its photoresponsive properties. The morphology of PMMAzo-b-PEG-b-PMMAzo in solvents was manipulated through the variation of the solvency and salt addition. Chun-Ming Wu (NSRRC) determined the detailed structures of PMMAzo-b-PEG-b-PMMAzo in selective solvents through small-angle neutron scattering (SANS).

In their experiments, PMMAzo-b-PEG-b-PMMAzo was dissolved in mixed *d*-DMF/D_2O solvents of concentration 3.9×10^{-6} M and then sealed in quartz cells. In the mixed solvents, *d*-DMF is a neutral solvent for the PEG and PMMAzo blocks, whereas D_2O is a PEG-selective solvent. The solvency thus altered when the solvent composition was varied. A SANS measurement was conducted at the **QUOKKA** beamline of Australian Centre for Neutron Scattering, Australia's Nuclear Science and Technology Organisation (ACNS, ANSTO).

Figure 1[1] shows SANS profiles of PMMAzo-b-PEG-b-PMMAzo in various mixed *d*-DMF/D_2O solvents. In the regions with large Q values, the SANS curves were approximated according to the spherical micelle form factor. By contrast, the increasing trend of intensity in regions with small Q values was attributed to the formation of micellar aggregates. The scattering curves of fractal aggregates were approximated with a simple power-law expression for the structure factor. Using a power-law expression for the regions with small Q values and the spherical micelle form factor for the regions with large Q values, they successfully predicted the morphologies that were formed by PMMAzo-b-PEG-b-PMMAzo in various mixed solvents (**Table 1**).[1]

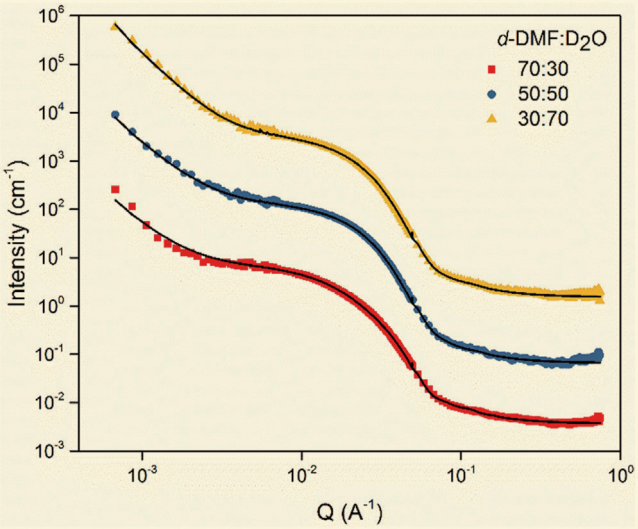

Fig. 1: SANS profiles of PMMAzo-b-PEG-b-PMMAzo in various mixed *d*-DMF/D_2O solvents measured at **Quokka**. [Reproduced from Ref. 1]

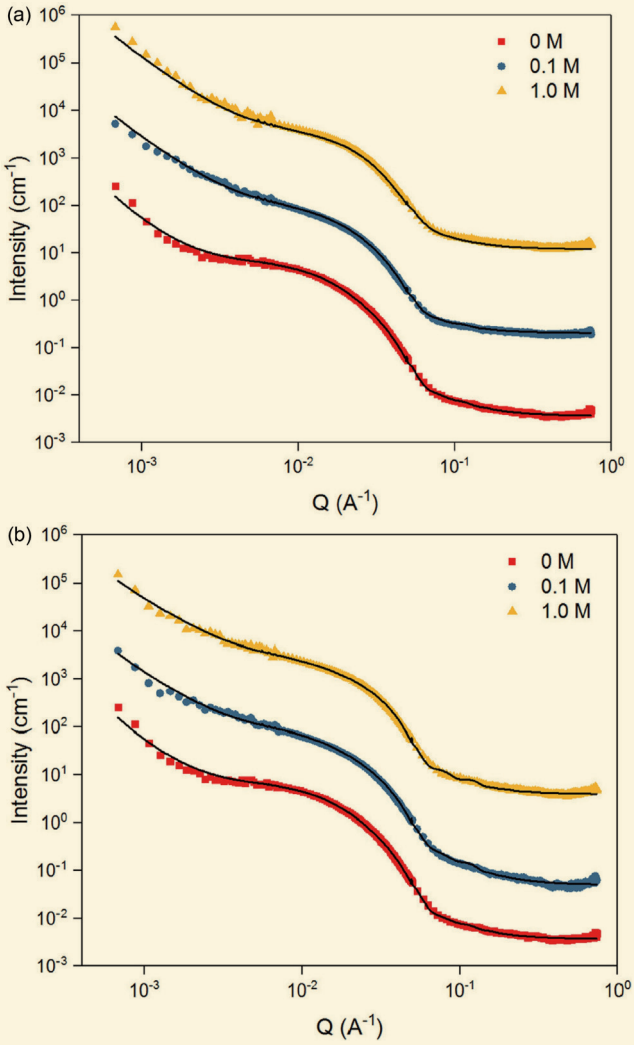

Fig. 2: SANS profiles of PMMAzo-b-PEG-b-PMMAzo in *d*-DMF/D_2O solvent 70:30 with varied concentration of (a) KCl and (b) KSCN measured at **Quokka**. [Reproduced from Ref. 1]

Table 1: Structural parameters of PMMAzo-b-PEG-b-PMMAzo in various mixed solvents. [Reproduced from Ref. 1]

d-DMF/D_2O composition	R_c (Å)	R_g (Å)	R_{total} (Å)	*n*	*M*
70:30	78.9	77.4	155.3	35.9	2.5
50:50	95.7	54.4	150.1	121.6	2.7
30:70	97.4	52.1	149.5	134.6	3.0

R_c: radius of micellar core; R_g: thickness of micellar corona; R_{total}: radius of micelles; *n*: association number of micelles; *M*: exponent of a power law.

Table 2: Structural parameters of PMMAzo-b-PEG-b-PMMAzo dissolved in *d*-DMF/D_2O solvent 70:30 with varied KCl concentration. [Reproduced from Ref. 1]

KCl concentration (M)	R_c (Å)	R_g (Å)	R_{total} (Å)	*n*	*M*
0	78.9	77.4	155.3	35.9	2.5
0.1	79.1	66.7	145.8	48.0	2.3
1.0	80.0	45.7	125.7	48.7	2.3

Table 3: Structural parameters of PMMAzo-b-PEG-b-PMMAzo dissolved in d-DMF/D_2O solvent 70:30 with varied KSCN concentration. [Reproduced from Ref. 1]

KSCN concentration (M)	R_c (Å)	R_g (Å)	R_{total} (Å)	*n*	*M*
0	78.9	77.4	155.3	35.9	2.5
0.1	78.5	81.5	160.0	34.2	2.2
1.0	77.2	82.5	159.7	33.8	2.1

Figure 2(a)[1] displays SANS profiles of PMMAzo-b-PEG-b-PMMAzo in *d*-DMF/D_2O solvent 70:30 with varied KCl concentration. As presented in **Table 2**,[1] the core radius marginally increased and the corona thickness considerably decreased when the KCl concentration was increased. This behavior was associated with the salting-out effect induced by KCl, which caused the dehydration of some ethylene oxide segments that were adjacent to the PEG/PMMAzo interface. The dehydrated ethylene oxide segments became hydrophobic and partly segregated into the micellar core, which resulted in an increased core radius. In contrast, the hydrophilic corona lost some dehydrated ethylene oxide segments, which caused a decreased corona thickness. In contrast to the salting-out effect induced by KCl, the solubility of PMMAzo segments in water increased upon the addition of KSCN. This effect facilitated their organization from the hydrophobic core to the hydrophilic corona in micelles and resulted in an increased corona thickness and a decreased core radius (**Fig. 2(b) and Table 3**).[1] (Reported by Chieh-Tsung Lo, National Cheng Kung University)

This report features the work of Chieh-Tsung Lo and his collaborators published in J. Mol. Liq. ***348****, 118013 (2022).*

ANSTO QUOKKA – Small-angle Neutron Scattering

- SANS
- Polymer, Biomaterial, Drug Delivery, Soft Matter

Reference

1. Y.-S. Wu, J.-Y. Ma, J. P. Mata, C.-M. Wu, K.-L. Hsu, C.-T. Lo, J. Mol. Liq. **348**, 118013 (2022).